JOC The Journal of Organic Chemistry

Article

pubs.acs.org/joc

Sesterterpenoids Isolated from the Sponge *Phorbas* sp. Activate Latent HIV-1 Provirus Expression

Meng Wang,[†] Ian Tietjen,[‡] Min Chen,[†] David E. Williams,[†] Julie Daoust,[†] Mark A. Brockman,[‡,§,∥] and Raymond J. Andersen*[,†]

[†]Departments of Chemistry and Earth, Oceans & Atmospheric Sciences, University of British Columbia, 2036 Main Mall, Vancouver, British Columbia, Canada V6T 1Z1

[‡]Faculty of Health Sciences, Simon Fraser University, Burnaby, British Columbia, Canada V5A 1S6

[§]British Columbia Centre for Excellence in HIV/AIDS, St. Paul's Hospital, Vancouver, British Columbia, Canada V6Z 1Y6

[∥]Department of Molecular Biology and Biochemistry, Simon Fraser University, Burnaby, British Columbia, Canada V5A 1S6

Supporting Information

ABSTRACT: Eight new sesterterpenoids, alotaketals D (**8**) and E (**9**), ansellones D (**10**), E (**11**), F (**12**), and G (**13**), and anvilones A (**14**) and B (**15**), have been isolated from extracts of the marine sponge *Phorbas* sp. collected in Howe Sound British Columbia, and their structures have been elucidated by analysis of NMR and MS data. Ansellone F (**12**) contains a rare 1,2−3,4-bis-epoxydecalin substructure. Anvilones A (**14**) and B (**15**) have an unprecedented tetracyclic anvilane terpenoid carbon skeleton. Using a cell culture model of latent HIV-1 infection, ansellone A (**3**), alotaketal D (**8**), and anvilone A (**14**) were found to induce HIV proviral gene expression similar to the control compound prostratin (**1**), while the known sesterterpenoid alotaketal C (**2**), isolated from the same extract, was more potent and gave a stronger response than prostratin (**1**). Like prostratin (**1**), all of the *Phorbas* sesterterpenoids with latency reversal agent properties appear to activate protein kinase C signaling.

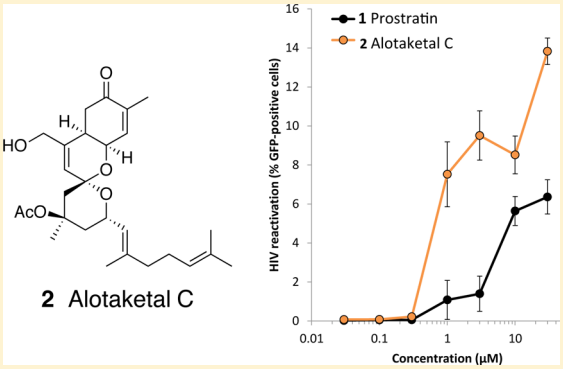

INTRODUCTION

Highly active antiretroviral therapy (HAART) has dramatically improved health outcomes for those infected with HIV-1, resulting in near normal life expectancy and quality of life. However, while HAART can reduce plasma virus loads to undetectable levels and limit onward transmission, it does not eliminate latent viral reservoirs that can re-establish productive infection if treatment is stopped. Thus, HAART is not curative and requires lifelong administration.[1−3]

Resting CD4+ T cells that contain integrated and transcriptionally silenced HIV-1 provirus represent a major reservoir of latent infection.[1,2] Activation of resting CD4+ T cells, often after prolonged periods of dormancy, leads to HIV-1 proviral gene expression and renewed viral infection. Thus, therapeutic strategies aimed at a sterilizing cure for HIV-1 have focused in large part on completely eliminating these latent proviruses. One potentially promising strategy, frequently termed "shock and kill", involves derepressing the transcription of HIV-1 proviruses in resting CD4+ T reservoir cells with small molecule drugs to produce replicating virus that can be inhibited by simultaneous administration of HAART. Activated T cells containing virus are eliminated by additional host or viral cytopathic effects, and released viral particles are inhibited by continued HAART administration.[4]

Several latency reversal agents (LRAs) have been identified that activate HIV-1 proviral gene expression through multiple mechanisms.[5,6] For example, histone deacetylase (HDAC), histone methyl transferase, and DNA methylation inhibitors have all been shown to activate latent HIV-1 in vitro, and HDAC inhibitors have been evaluated in clinical trials in combination with HAART.[4] A number of natural product activators of protein kinase C (PKC), including the polyketide bryostatin-1[6] and the diterpenoid prostratin (**1**), induce translocation of the host cell transcription factor NF-$\kappa\beta$ from the cytoplasm, where it is sequestered in resting cells, to the nucleus where it activates transcription of HIV-1 genes. However, to date, no single LRA from any functional class has shown reduction in the size of the latent viral reservoir of HIV-1 infected patients in vivo. Therefore, it has been suggested that combinations of LRAs acting via different mechanisms and with increased potency compared with the currently available agents will be needed to realize the promise of the "shock and kill' approach to a sterilizing HIV-1 cure.[6]

As part of a program designed to find natural products that may serve as new LRAs, we have used a Jurkat helper T cell line

Received: September 20, 2016
Published: October 21, 2016

DOI: 10.1021/acs.joc.6b02312
J. Org. Chem. 2016, 81, 11324−11334

Chart 1

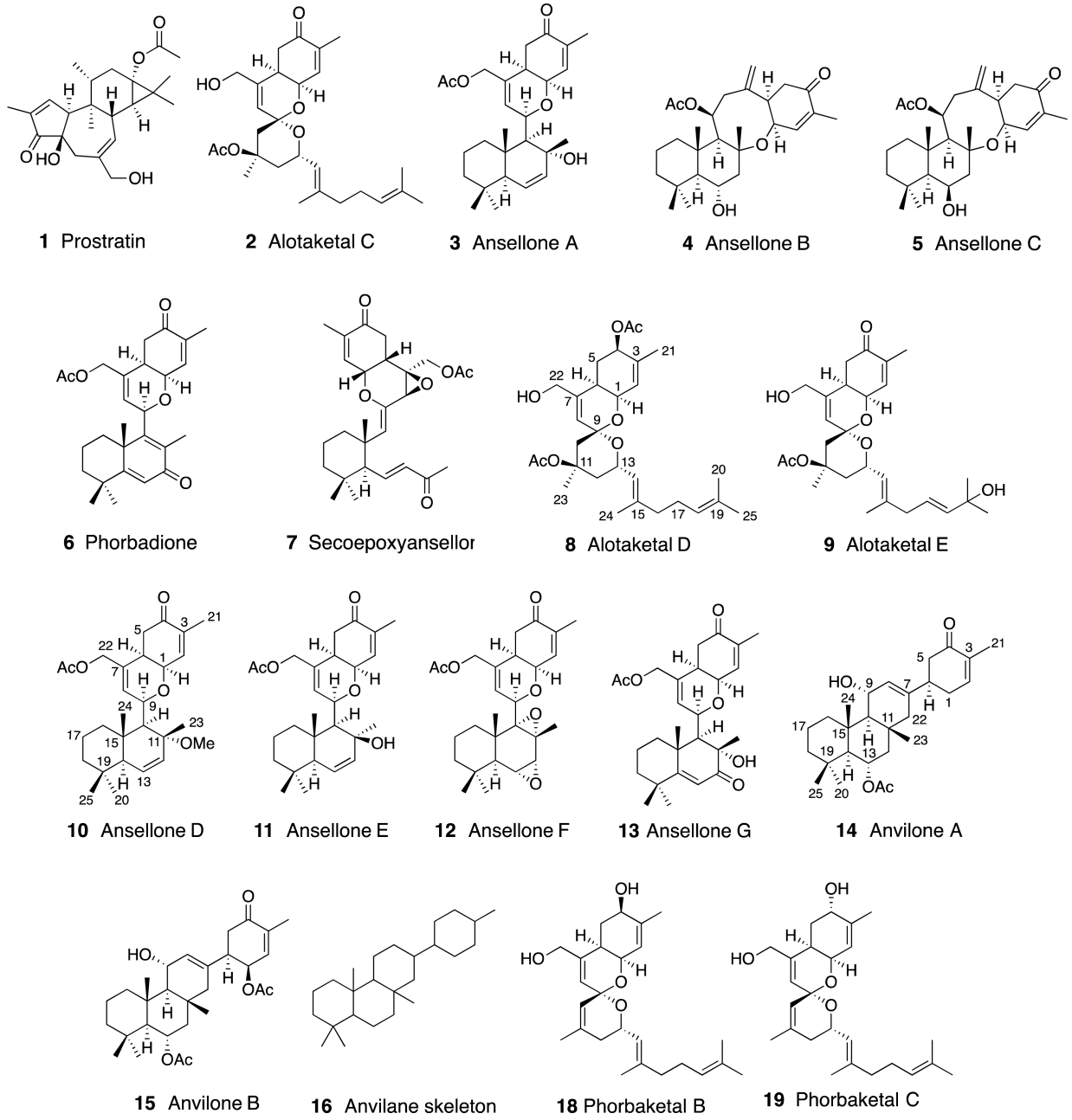

(JLat 9.2), which encodes an integrated noninfectious HIV-1 provirus containing a GFP reporter sequence,[7] to screen our library of pure marine natural products. GFP expression in the assay is an indicator of proviral gene expression, and prostratin (**1**) was used as a positive control LRA. Preliminary data suggested that the sesterterpenoid alotaketal C (**2**) isolated from the marine sponge *Phorbas* sp. collected in British Columbia[8,9] gave a stronger response in this assay than the positive control prostratin (**1**) (e.g., 13.8 ± 2.2% vs 6.4 ± 3.2% GFP-positive cells for 30 μM of **2** and **1**, respectively; Table SI1, Supporting Information). Prompted by this encouraging result, we carried out an exhaustive search for minor sesterterpenoid components in the *Phorbas* sp. crude extract. This effort has resulted in the reisolation of the six already reported sesterterpenoids alotaketal C (**2**),[8,9] ansellones A (**3**),[10] B (**4**), and C (**5**), phorbadione (**6**), and secoepoxyansellone A (**7**),[8,10] along with the eight new sesterterpenoids alotaketals D (**8**) and E (**9**), ansellones D (**10**), E (**11**), F (**12**), and G (**13**), anvilone A (**14**), and anvilone B (**15**) (Chart 1). Anvilones A (**14**) and B (**15**) have the unprecedented "anvilane" sesterterpenoid carbon skeleton **16**. Members of this family of sesterterpenoids showed a wide range of activities in the LRA screening assay, from complete inactivity to activity greater than prostratin (**1**), which has revealed some preliminary SAR. Additional cell-based studies further implicate these sesterterpenoids, like prostratin (**1**), as members of the PKC-activator class of LRAs. The details of the structure elucidation of the new compounds **8**–**15**, their activities in the LRA assay, a discussion of the SAR for the LRA pharmacophore(s), and a biogenetic proposal for the formation of the unprecedented anvilane carbon skeleton **16** are presented below.

DOI: 10.1021/acs.joc.6b02312
J. Org. Chem. 2016, 81, 11324–11334

Table 1. NMR Data for Alotaketal C (2),[8] Alotaketal D (8), and Alotaketal E (9) Recorded in C_6D_6 at 600 MHz

	alotaketal C (2)		alotaketal D (8)		alotaketal E (9)	
C no.	δ_C	δ_H (J, Hz)	δ_C	δ_H (J, Hz)	δ_C	δ_H (J, Hz)
1	63.2	4.27 (dd, 3.2, 4.9)	63.5	4.27 (br t, 4.3)	63.3	4.24 (dd, 3.4, 4.9)
2	139.1	6.27 (dd, 1.2, 5.6)	125.5	5.61 (dt, 5.2, 1.6)	139.3	6.25 (dd, 5.7, 1.4)
3	138.6		140.2		138.9	
4	197.7		72.3	5.39 (dd, 10.1, 5.6)	197.3	
5	38.5	2.38 (d, 8.8)	29.0	1.71 (q, 11.3)	38.5	2.37 (d, 8.5)
5′		2.38 (d, 8.8)		2.00 (ddd, 11.5, 5.8, 1.6)		2.37 (d, 8.5)
6	34.1	1.99 (td, 3.2, 9.0)	33.2	1.77 (m)	34.0	1.98 (dt, 3.3, 8.5)
7	142.4		142.7		142.6	
8	125.2	5.44 (br s)	125.7	5.52 (br s)	125.0	5.41 (br s)
9	96.8		96.3		96.7	
10	39.9	3.11 (dd, 14.7, 2.2)	40.3	3.16 (dd, 14.6, 2.3)	39.9	3.11 (dd, 14.6, 2.3)
10′		1.19 (d, 14.7)		1.25 (d, 14.7)[a]		1.19 (d, 14.6)
11	77.4		77.6		77.4	
12	44.1	1.19 (d, 14.0)	44.3	1.23 (dd, 14.8, 11.2)[a]	44.0	1.20 (m)
12′		1.81 (dt, 1.1, 14.0)		1.83 (dt, 2.1, 13.7)		1.80 (td, 2.2, 13.9)
13	64.0	5.13 (m, 1.1, 14.0)	63.8	5.19 (ddd, 11.2, 8.2, 2.0)[b]	64.0	5.12 (ddd, 11.2, 8.2, 2.0)
14	126.4	5.46 (d, 10.0)	126.6	5.47 (dd, 8.2, 1.0)	127.3	5.45 (dq, 8.2, 1.1)
15	139.4		139.1		137.9	
16	40.2	2.11 (dt, 8.3)	40.3	2.10 (br t, 7.7)	43.1	2.68 (br d, 5.9)
17	27.3	2.21 (m)	27.3	2.20 (m)	128.5	5.63 (m)
18	124.7	5.23 (br t, 6.9)	124.9	5.22 (dt, 7.0, 1.4)[b]	137.1	5.62 (d, 15.8)
19	132.0		131.8		81.8	
20	18.1	1.55 (s)	18.1	1.54 (s)	24.9	1.22 (s)
21	16.3	1.77 (s)	19.1	1.63 (s)	16.3	1.77 (s)
22	63.7	3.51 (m)	64.0	3.65 (m)	63.7	3.49 (m)
23	27.3	1.45 (s)	27.5	1.47 (s)	27.3	1.43 (s)
24	17.2	1.77 (s)	17.2	1.79 (d, 0.9)	17.2	1.75 (d, 1.0)
25	26.2	1.67 (s)	26.2	1.66 (br s)	24.9	1.22 (s)
26	170.4		170.0		170.1	
27	22.4	1.77 (s)	20.1	1.66 (br s)	22.4	1.77 (s)
28			170.0			
29			22.7	1.93 (s)		
OH		0.58 (s)		0.60 (br s)		0.52 (t, 5.7)

[a]Overlapped. [b]Overlapped.

RESULTS AND DISCUSSION

Fresh specimens of the *Phorbas* sp. were collected by hand using SCUBA along the rocky shoreline in Howe Sound British Columbia and extracted with MeOH as previously described.[8] The concentrated MeOH extracts were partitioned between H_2O and EtOAc followed by subjecting the EtOAc-soluble materials to sequential application of Sephadex LH20 and reversed-phase HPLC chromatographies to give pure samples of the known and new sesterterpenoids **2** to **15**.

Preliminary examination of the NMR data for the new sesterterpenoids showed that two of them were closely related to alotaketal C (**2**) (Table 1 and Supporting Information). Alotaketal D (**8**) was obtained as a white powder that gave a $[M + Na]^+$ ion in the ESITOFHRMS at m/z 525.2827 consistent with a molecular formula of $C_{29}H_{42}O_7$ (calcd for $C_{29}H_{42}O_7Na$ 525.2828), which required nine sites of unsaturation. Comparison of the ^1H and ^{13}C NMR data collected for **8** with the corresponding NMR data obtained for **2** (Table 1) showed that **8** contained the same bicyclic spiroketal core fragment (C-6 to C-13 and C-1) and C-14 to C-20 side chain found in **2**. The differences in the NMR data for **8** and **2** were in the resonances assigned to the C-2 to C-4 region of the C-1 to C-6 cyclohexene ring in **2** (Table 1). COSY correlations were observed between a resonance at δ 4.27, assigned to H-1 in **8**, and resonances at δ 5.61 and 1.77 assigned to H-2 and H-6, respectively. Additional COSY correlations were observed between H-2 (δ 5.61) and a methyl resonance at δ 1.63 assigned to Me-21, between H-6 (δ 1.77) and a pair of germinal methylene resonances at δ 1.71 and 2.00 assigned to H-5 and H-5′, and between H-5 and H-5′ and a deshielded methine resonance at δ 5.39 assigned to H-4. The upfield shift of H-2, the presence of a deshielded methine at C-4 (δ 72.3), and the absence of a ketone carbonyl resonance in the ^{13}C NMR of **8** indicated that the C-4 ketone in **2** had been replaced by an oxymethine in **8**. HMBC correlations observed between a deshielded ^{13}C resonance at δ 170.0, assigned to an ester, and both the H-4 methine at δ 5.39 and a methyl singlet at δ 1.66, established the presence of an acetate ester substituent at C-4, completing the assignment of the constitution of **8**.

Analysis of the ROESY and coupling constant data obtained for **8** confirmed that it had the same relative configurations at C-1, C-6, C-9, C-11, and C-13 as **2**, and a biogenetic argument led to the assumption that **8** also has the same absolute configurations at these centers as **2**. The H-4 resonance at δ 5.39 was a dd with J = 10.1 and 5.6 Hz, indicating that it was pseudoaxial with one anti and one gauche coupling partner.

DOI: 10.1021/acs.joc.6b02312
J. Org. Chem. 2016, 81, 11324−11334

The H-5 resonance at δ 1.71 in **8** was partly obscured but clearly had at least two coupling constants of $J \approx 10-11.3$ Hz and no couplings of $J = 5.6$ Hz, and the H-5′ resonance at δ 2.00 was a ddd with coupling constants of 11.5, 5.8, and 1.6 Hz. These data were consistent with H-4, H-5, and H-6 all being pseudoaxial and H-5′ being pseudoequatorial. Therefore, the acetate substituent at C-4 was assigned as pseudoequatorial and *trans* to H-6 as shown in **8**. In support of this assignment, the corresponding carbinol methine proton in phorbaketal A (**18**),[11] which has the same relative configuration as that assigned to alotaketal D (**8**), is reported to be a bd with $J = 10.3$ Hz, and phorbaketal C (**19**), that is epimeric at C-4 compared with **8**, has a carbinol methine signal that is a dd with $J = 3.7$ and 2.0 Hz. Finally, a ROESY correlation was observed between the H-4 (δ 5.39) and H-6 (δ 1.77) resonances in alotaketal D (**8**) in agreement with both protons being pseudoaxial and *cis*.

Alotaketal E (**9**) was isolated as a white powder that gave an $[M + Na]^+$ ion in the ESITOFHRMS at m/z 513.2452 consistent with a molecular formula of $C_{27}H_{38}O_8$ (calcd for $C_{27}H_{38}O_8Na$ 513.2464), which differed from the molecular formula of alotaketal C (**2**) by addition of a single oxygen atom. Comparison of the 1D and 2D NMR data acquired for alotaketals C (**2**) and E (**9**) (Table 1 and Supporting Information) showed that they contained identical C-1 to C-13 tricyclic cores and C-14, C-15, and C-16 functionalities, differing only in the C-17 to C-20 region of their side chains. HMBC correlations observed between a six-proton singlet at δ 1.22 (Me-20 and Me-25) and carbon resonances at δ 24.9 (Me-20, Me-25), 81.8 (C-19), and 137.1 (C-18) identified a pair of germinal methyls attached to an oxygenated tertiary carbon, which was in turn attached to an olefinic methine carbon. An HSQC correlation was observed between the olefinic carbon at δ 137.1 (C-18) and a proton doublet ($J = 15.8$ Hz) at δ 5.62 (H-18), which showed a COSY correlation to a complex olefinic resonance at δ 5.63, assigned to H-17. The H-17 (δ 5.63) resonance showed a COSY correlation to a broad two proton doublet at δ 2.68 (J = 5.9 Hz), assigned to H-16/H-16′. An ESILRMS recorded on **9** dissolved in MeOD gave a $[M + Na]^+$ ion at m/z 515.3 compared with the $[M + Na]^+$ ion at m/z 513.3 for **9** dissolved in MeOH, demonstrating the presence of two exchangeable protons in **9**. Therefore, the oxygen substituent at C-19 had to be an alcohol, and the 15.8 Hz coupling observed between H-17 and H-18 revealed that the $\Delta^{17,18}$ olefin had the *E* configuration shown in **9**.

Preliminary examination of the NMR data collected for four of the new sesterterpenoids showed that they were closely related to ansellone A (**3**)[10] (Tables 2 and 3 and Supporting Information). Ansellone D (**10**), the first of these new ansellone A analogues, gave an $[M + Na]^+$ ion at m/z 479.2778 in the ESITOFHRMS appropriate for a molecular formula of $C_{28}H_{40}O_5$ (calcd for $C_{28}H_{40}O_5Na$ 479.2773), which differed from the molecular formula of ansellone A (**3**) by addition of CH_2. The major difference in the 1D and 2D NMR data obtained for ansellone D (**10**) compared with the NMR data obtained for ansellone A (**3**) (Tables 2 and 3) was the presence of a methyl singlet at δ 3.04 (Me-28), assigned to a methyl ether, in the ^{1}H NMR spectrum of **10**. There were also noticeable differences in the chemical shifts of H-10 (δ 1.46 in **3**; 1.82 in **10**), H-12 (δ 5.52 in **3**; 5.45 in **10**), H-13 (δ 5.59 in **3**; 5.81 in **10**), and Me-23 (δ 1.50 in **3**; 1.61 in **10**) indicating that the structural difference between **3** and **10** was located in the C-10 to C-13 region of the molecules. HMBC correlations were observed between a carbon resonance at δ 78.4, assigned to C-11, and Me-23 (δ1.61), H-10 (δ 1.82), and H-13 (δ 5.81). The C-11 (δ 78.4) resonance also showed a strong HMBC correlation to the methyl ether resonance at δ 3.04 (Me-28) indicating that ansellone D (**10**) just differed from ansellone A (**3**) by the presence of a methyl ether rather than a hydoxy substituent at C-11. The ^{13}C chemical shift of Me-23 in ansellone D (**10**) (δ 25.5) was nearly identical to the chemical shift of Me-23 in **3** (δ 26.5), confirming that Me-23 was also axial in **10** as shown.

Ansellone E (**11**) was isolated as a white powder that gave a $[M + Na]^+$ ion in the ESITOFHRMS at m/z 465.2615 consistent with a molecular formula of $C_{27}H_{38}O_5$ (calcd for $C_{27}H_{38}O_5Na$ 465.2617), which is identical to the molecular formula of ansellone A (**3**). Analysis of the 1D and 2D NMR data obtained for ansellone E (**11**) (Tables 2 and 3 and Supporting Information) showed that it had the same constitution as ansellone A (**3**). Significant differences in the NMR data for **11** and **3** were again only observed in the ^{1}H chemical shifts of H-10 (δ 1.46 in **3**; 1.33 in **11**), H-12 (δ 5.52 in **3**; 5.85 in **11**), and Me-23 (δ 1.50 in **3**; 1.35 in **11**) and the ^{13}C chemical shift of Me-23 (δ 26.5 in **3**; 31.4 in **11**). The ^{13}C chemical shift of Me-23 in **11** (δ 31.4) indicated that it was in an equatorial orientation compared with its axial orientation in **3**. Therefore, ansellone E was assigned the structure shown in

Table 2. ^{13}C NMR Data for Ansellone A (3),[10] Ansellone D (10), Ansellone E (11), Ansellone F (12), and Ansellone G (13) Recorded in C_6D_6 at 150 MHz

	ansellone A **3**	ansellone D **10**	ansellone E **11**	ansellone F **12**	ansellone G **13**
C no.	δ_C	δ_C	δ_C	δ_C	δ_C
1	70.9	70.5	70.9	70.8	70.5
2	139.4	139.1	138.8	138.7	139.4
3	138.6	138.2	139.0	139.1	139.0
4	197.7	197.5	197.2	197.2	197.6
5	38.6	38.3	38.7	38.5	39.0
6	34.8	34.5	34.9	34.7	34.7
7	131.4	131.1	131.7	132.2	131.3
8	134.8	134.8	133.3	128.7	133.6
9	76.9	76.2	77.5	78.2	76.7
10	63.8	55.4	61.5	69.7	59.3
11	73.1	78.4	71.7	60.4	75.5
12	135.7	132.3	136.2	53.6	203.3
13	128.0	131.7	125.9	49.8	120.2
14	57.0	56.7	55.9	46.7	180.3
15	42.1	42.0	39.7	41.2	43.1
16	38.9	38.9	39.4	35.8	40.7
17	18.9	18.5	18.9	19.0	17.8
18	41.7	41.3	41.7	41.1	40.0
19	33.1	32.7	33.3	33.3	37.8
20	33.6	33.2	33.6	33.4	32.7
21	16.3	15.9	16.3	16.3	16.3
22	66.1	65.8	66.1	65.6	66.0
23	26.5	25.5	31.4	19.0	25.5
24	16.8	17.0	16.6	18.9	23.4
25	22.2	21.8	22.4	22.7	30.1
26	170.2	169.9	169.9	170.0	170.3
27	20.8	20.4	20.7	20.6	20.7
28		49.2			

DOI: 10.1021/acs.joc.6b02312
J. Org. Chem. 2016, 81, 11324−11334

Table 3. ^{1}H NMR Data for Ansellone A (3),[10] Ansellone D (10), Ansellone E (11), Ansellone F (12), and Ansellone G (13) Recorded in C_6D_6 at 600 MHz

	ansellone A (3)	ansellone D (10)	ansellone E (11)	ansellone F (12)	ansellone G (13)
C no.	δ_H (J, Hz)	δ_H (J, Hz)	δ_H (J, Hz)	δ_H (J, Hz)	δ_H (J, Hz)
1	3.44 (br t, 4.8)	3.44 (t, 4.2)	3.50 (t, 4.3)	3.38 (br t, 4.1)	3.46 (t, 4.4)
2	6.14 (d, 4.8)	6.14 (dd, 5.6, 1.2)	6.03 (dd, 5.6, 1.3)	6.14 (dd, 5.5, 1.2)	6.13 (dd, 5.6, 1.4)
3					
4					
5	2.67 (d, 9.0)	2.68 (m)	2.65 (m)	2.63[a]	2.67 (dd, 15.9, 4.3)
5′	2.67 (d, 9.0)	2.68 (m)	2.65 (m)	2.63[a]	2.57 (dd, 15.9, 13.1)
6	2.10 (tt, 9.0, 3.0)	2.09 (t, 8.2)	2.05 (dt, 7.1, 2.9)	2.04 (m)	1.99 (dm, 12.9)
7					
8	5.70 (br s)	5.68 (br s)	5.72 (br s)	5.99 (br s)	5.58 (br s)
9	4.77 (br s)	4.69 (br s)	4.76 (br s)	4.12 (br s)	5.15 (m)
10	1.46 (br s)	1.82 (br s)	1.33 (m)		1.92 (d, 1.4)
11					
12	5.52 (dd, 10.0, 3.0)	5.45 (dd, 10.3, 3.1)	5.85 (dd, 10.1, 3.0)	2.80 (d, 4.4)	
13	5.59 (br d, 10.0)	5.81 (dd, 10.3, 1.5)	5.57 (dd, 10.1, 1.7)	2.65[a]	6.08 (s)
14	1.71 (m)	1.71 (m)	1.50 (t, 2.4)	1.80 (d, 4.6)	
15				1.20 (m)	
16	1.02 (m)	1.09 (m)[a]	0.96 (dt, 12.8, 3.3)	1.27 (dd, 12.3, 3.9)	0.93 (dt, 13.4, 4.1)
16′	1.82 (br d, 13.0)	1.87 (bd, 12.8)	1.82 (dt, 12.5, 3.3)	1.84 (dt, 13.1, 3.5)	1.94 (m)
17	1.33 (m)	1.35 (m)	1.36 (m)	1.38 (m)	1.21 (m)
17′	1.53 (dt, 13.0, 3.5)	1.56 (dm, 13.7)	1.54 (dt, 13.7, 3.2)	1.34 (m)	1.46 (m)
18	1.04 (m)	1.09 (m)[a]	1.06 (td, 13.5, 3.9)	0.98 (m)	1.06 (m)
18′	1.29 (m)	1.31 (dm, 13.2)	1.33 (m)	1.20 (m)	1.15 (m)
19					
20	0.86 (s)	0.85 (s)	0.86 (s)	1.00 (s)	0.85 (s)
21	1.69 (s)	1.69 (s)	1.68 (s)	1.71 (s)	1.73 (s)
22	4.27 (br d, 12.0)	4.25 (br d, 12.4)	4.25 (br d, 12.6)	4.21 (br d, 13.0)	4.19 (br d, 12.7)
22′	4.42 (br d, 12.0)	4.43 (br d, 12.4)	4.38 (br d, 12.6)	4.35 (br d, 13.0)	4.32 (br d, 12.8)
23	1.50 (s)	1.61 (s)	1.35 (s)	1.40 (s)	1.63 (s)
24	1.20 (s)	1.26 (s)	1.31 (s)	1.21 (s)	1.47 (s)
25	0.78 (s)	0.78 (s)	0.83 (s)	0.81 (s)	0.87 (s)
26					
27	1.67 (s)	1.65 (s)	1.66 (s)	1.64 (s)	1.64 (s)
28		3.04 (s)			
OH		3.23 (br s)			3.83 (s)

[a]Overlapped resonances.

11, which is simply epimeric at C-11 compared with ansellone A (**3**).

Ansellone F (**12**), isolated as a white powder, gave a $[M + Na]^+$ ion in the ESITOFHRMS at m/z 479.2403 in agreement with a molecular formula of $C_{27}H_{36}O_6$ (calcd for $C_{27}H_{36}O_6Na$ 479.2410), which required 10 sites of unsaturation and differed from the molecular formula of ansellone A (**3**) by the loss of two hydrogen atoms and the addition of one oxygen atom. Analysis of the 1D and 2D NMR data obtained for ansellone F (**12**) showed that it had the identical C-1−C-9 $C_{13}H_{15}O_4$ bicyclic fragment found in ansellone A (**3**) (Tables 2 and 3), which accounted for six sites of unsaturation and all of the carbonyl and alkene resonances in the ^{13}C NMR spectrum of **12**. Therefore, the remaining $C_{14}H_{21}O_2$ fragment of **12** had to be tetracyclic. HSQC and APT data obtained for **12** revealed that the $C_{14}H_{21}O_2$ fragment contained four methyl, three methylene, three methine, and four quaternary carbons, which showed that all 21 hydrogen atoms were attached to carbon, and therefore, the two oxygen atoms had to be ether linkages.

HMBC correlations observed between both of the methyl singlets at δ 0.81 (Me-25) and 1.00 (Me-20) and carbon resonances at δ 33.3 (C: C-19), 41.1 (CH_2: C-18), and 46.7 (CH: C-14) identified a fragment consisting of a pair of germinal methyls attached to a quaternary carbon that was in turn attached to methylene and methine carbons. A third methyl singlet at δ 1.21 (Me-24) showed HMBC correlations to the methine carbon resonance at δ 46.7 (C-14), to an overlapped resonance at δ 41.2 (C: C-15), and to additional resonances at δ 35.8 (CH_2: C-16) and 69.7 (C: C-10), demonstrating that the methine carbon (C-14) was linked to both of the quaternary carbons (C-19 and C-15) bearing the methyls. HSQC correlations showed that the methylene carbon resonating at δ 35.8 (C-16) was attached to hydrogen atoms with resonances at δ 1.27 (H-16) and 1.84 (H-16′), the methylene carbon resonating at δ 41.1 (C-18) was attached to hydrogen atoms with resonances at δ 0.98 (H-18) and 1.20 (H-18′), and the third methylene carbon resonating at δ 19.0 (C-17) was attached to hydrogen atoms with resonances at δ 1.38 (H-17) and 1.34 (H-17′). COSY correlations established that the three methylene carbons were connected to form the C-14 to C-19 cyclohexane ring bearing three methyl substituents (Me-20, Me-24, Me-25) that is present in all of the other ansellones A to E.

DOI: 10.1021/acs.joc.6b02312
J. Org. Chem. 2016, 81, 11324−11334

The remaining $C_5H_5O_2$ fragment of ansellone F (**12**) had to account for carbon/proton resonances at δ 69.7 (C-10), 60.4 (C-11), 53.6/2.80 (CH-12), 49.8/2.65 (CH-13), and 19.0/1.40 (Me-23), three rings, and two ethers. A COSY correlation observed between the two methine protons (δ 2.80, H-12; 2.65, H-13) showed that the methine carbons were vicinal and their ^{13}C NMR chemical shifts (δ 53.6 and 49.8) indicated that they were part of an epoxide functionality, which required that the remaining two nonprotonated carbons at δ 69.7 (C-10) and 60.4 (C-11) and the final oxygen atom must also be part of an epoxide functionality. HMBC correlations observed between the methyl resonance at δ 1.40 (Me-23) and the carbon resonances at δ 53.6 (C-12), 69.7 (C-10), 60.4 (C-11) showed that the two epoxides were linked through the methine carbon at δ 53.6 (C-12) and one of the two carbons at δ 69.7 (C-10) and 60.4 (C-11), and that the methyl group (C-23) was also attached to one of these two nonprotonated carbons. Additional HMBC correlations observed between the methyl resonance at δ 1.21 (Me-24) and the epoxide resonance at δ 69.7 (C-10), and between the H-14 methine resonance at δ 1.80 and both of the epoxide carbon resonances at δ 69.7 (C-10) and 49.8 (C-13), showed that the four carbon bis epoxide fragment was fused to C-15 via a nonprotonated epoxide carbon (C-10) and to C-14 via an epoxy methine carbon (C-13), which required that the methyl group (Me-23) resonating at δ 1.40 had to be attached to the internal nonprotonated epoxy carbon (C-11) resonating at δ 60.4 (C-11). A COSY correlation observed between H-13 (δ 2.65) and H-14 (δ 1.80) confirmed this assignment to complete the constitution for ansellone F as shown in **12**.

A ROESY correlation observed between the Me-24 and Me-25 resonances at δ 1.21 and 0.81 in **12** demonstrated that the methyl groups were both axial and that the decalin rings were *trans* fused. Additional ROESY correlations observed between the H-13 methine resonance at δ 2.65 and both of the Me-24 (δ 1.21) and Me-25 (δ 0.81) resonances indicated that H-13 was *cis* to the two axial methyls. A ROESY correlation observed between the Me-24 resonance (δ 1.21) and the H-8 resonance at δ 5.99 indicated that C-9 and Me-24 were also *cis* as shown in **12**. We have assumed that the absolute configurations at C-1, C-6, C-9, C-14, and C-15 are identical in ansellone A (**3**) and ansellone F as shown in **12**.

Ansellone G (**13**) was isolated as a white powder that gave a $[M + Na]^+$ ion in the ESITOFHRMS at m/z 479.2409 (calcd for $C_{27}H_{36}O_6Na$ 479.2410) consistent with a molecular formula of $C_{27}H_{36}O_6$, that required 10 sites of unsaturation. Analysis of the 1D and 2D NMR data obtained for ansellone G (**13**) (Tables 2 and 3 and Supporting Information) showed that it had the identical C-1−C-9 $C_{13}H_{15}O_4$ bicyclic fragment and the same C-10/C-11/Me-23 and C-15 to C-20/Me-24/Me-25 functionalities found in ansellone A (**3**), which accounted for six sites of unsaturation. The ^{13}C NMR spectrum recorded for **13** contained additional olefinic methine and nonprotonated olefinic carbon resonances at δ 120.2 (C-13) and 180.3 (C-14), along with a shielded ketone carbonyl resonance at δ 203.3 (C-12), which could be assigned to an $\alpha\beta$-unsaturated ketone fragment. HMBC correlations observed between the Me-23 resonance at δ 1.63 and the ketone carbonyl resonance at δ 203.3 (C-12) and between the Me-20, Me-24, and Me-25 resonances at δ 0.85, 1.47, and 0.87, respectively, and the olefinic resonance at δ 180.3 (C-14) placed the ketone functionality at C-12 and the $\alpha\beta$ olefinic carbons at C-13 and C-14, completing the constitution of **13**. The ROESY data recorded for ansellone G (Supporting Information) confirmed that Me-24 (δ 1.47) and Me-25 (δ 0.87) were both axial, and the chemical shift of Me-23 (δ 25.5) indicated that it was also axial. Therefore, the relative configuration of ansellone G was assigned as shown in **13**.

Anvilone A (**14**) was isolated as a colorless powder that showed a $[M + Na]^+$ ion in the ESITOFHRMS spectrum at m/z 451.2823 appropriate for a molecular formula of $C_{27}H_{40}O_4$ (calcd for $C_{27}H_{40}O_4Na$ 451.2824) requiring eight sites of unsaturation. The ^{13}C NMR spectrum of **14** contained four olefinic resonances (δ 125.3, C-8; 138.5, C-7; 135.6, C-3; 142.9, C-2) and two carbonyl resonances (δ 169.5, 13-OAc; 197.7, C-4) (Table 4 and Supporting Information) accounting for four sites of unsaturation, indicating that **14** had to be tetracyclic. Detailed analysis of the COSY and HMBC data recorded for anvilone A (**14**) as shown in **a**, **b**, **c**, and **d** of Figure 1 identified two fragments **A** and **B** that resembled the C-1−C-6 methylcyclohexenone and C-10−C-20/Me-23/Me-24/Me-25

Table 4. NMR Data for Anvilone A (14) and Anvilone B (15) Recorded in C_6D_6 at 600 MHz

	anvilone A (**14**)		anvilone B (**15**)	
C no.	δ_C	δ_H (J, Hz)	δ_C	δ_H (J, Hz)
1	30.4	1.80 (dd, 12.1, 3.8)	66.7	5.26 (br t, 4.4)
1′		1.67 (m)		
2	142.9	6.11 (dm, 4.9)	138.6	6.47 (dd, 5.5, 1.4)
3	135.6		138.5	
4	197.7		197.6	
5	42.8	2.40 (dd, 15.4, 2.0)	38.2	2.67 (dd, 16.2, 12.7)
5′		2.02 (dd, 14.4,13.4)		2.34 (dd, 16.2, 3.5)
6	41.7	2.11[a]	43.2	2.18 (m)
7	138.5		135.0	
8	125.3	5.03 (br s)	128.3	5.10 (br dt, 3.0, 1.0)
9	67.1	3.93 (br s)	67.6	3.98 (br t, 8.2)
10	60.4	0.82 (d, 8.9)	60.5	0.87 (d, 8.9)
11	36.9		37.2	
12	49.6	1.24 (m)	50.0	1.27 (m)[a]
12′		1.80 (m)		1.79 (m)
13	70.4	5.44 (dt, 3.8, 11.2)	70.5	5.46 (dt, 3.8, 11.2)
14	59.2	1.21 (m)	59.7	1.25 (m)[a]
15	40.9		41.3	
16	41.8	2.13[a]	42.2	2.18 (m)
16′		1.11 (m)[b]		1.12 (m)
17	18.7	1.55 (m)	19.1	1.56 (dm, 13.8)
17′		1.39 (dm, 13.4)		1.40 (dm, 13.8)
18	44.0	1.33 (m)	44.3	1.33 (m)
18′		1.27 (dd, 13.4, 4.4)		1.27 (m)[a]
19	33.6		33.9	
20	37.0	1.22 (s)	37.4	1.23 (s)
21	16.0	1.85 (s)	16.0	1.75 (s)
22	46.7	1.51 (br d, 17.0)	47.6	1.51 (br d, 16.4)
22′		1.10 (br d, 17.0)[b]		1.32 (m)
23	22.3	0.80 (s)	22.4	0.85 (s)
24	17.5	0.96 (s)	17.9	0.99 (s)
25	22.4	0.98 (s)	22.8	1.00 (s)
26	169.5		169.3	
27	21.6	1.78 (s)	20.4	1.62 (s)
28			169.3	
29			22.0	1.79 (s)
OH		0.37 (d, 8.6)		0.41

[a]Overlapped resonances. [b]Overlapped resonances.

DOI: 10.1021/acs.joc.6b02312
J. Org. Chem. 2016, 81, 11324−11334

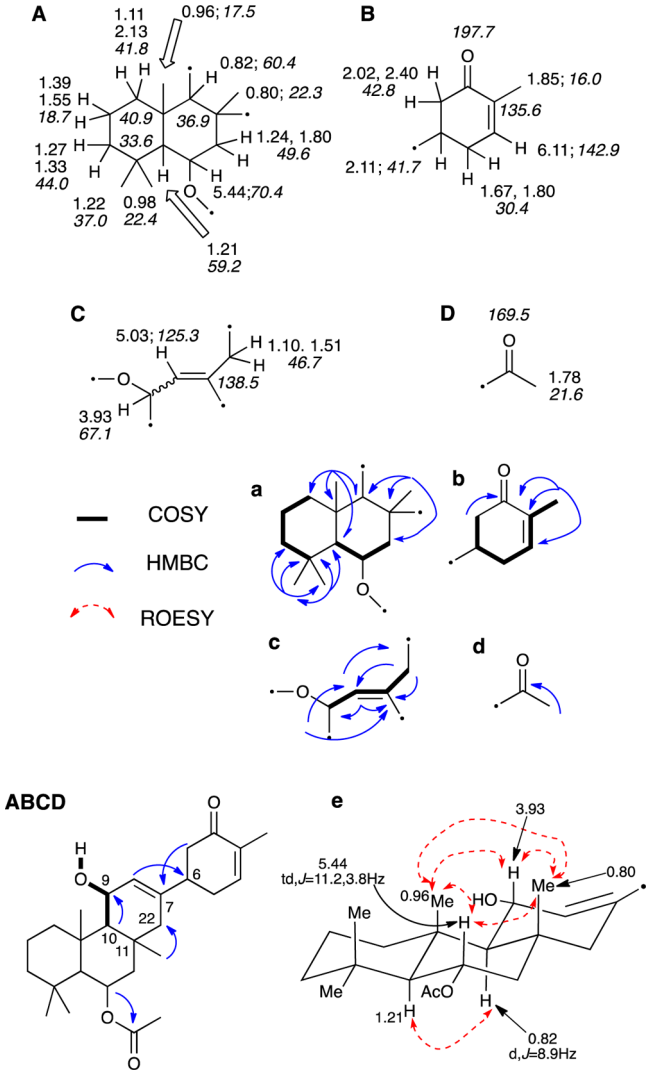

Figure 1. Fragments of anvilone A (**14**) with ^{1}H and ^{13}C NMR assignments and important COSY, HMBC, and ROESY correlations shown.

decalin fragments found in ansellone A (**3**), accounting for three of the four required rings. A third fragment **C** (Figure 1), although differing in functionality, had a four-carbon skeleton that matched the C-7 to C-9/C-22 moiety that linked the decalin and cyclohexenone fragments in ansellone A (**3**). The NMR data also identified an acetyl residue in **14** as shown in Figure 1 panels **D**/**d**.

A series of HMBC and COSY correlations identified the bonds that link fragments **A**–**D** together to give the complete constitution of anvilone A (**14**) as shown in Figure 1 (**A**–**D**). A COSY correlation observed between the fragment **A** methine at δ 0.82 (H-10) and the fragment **C** oxymethine resonance at δ 3.93 (H-9) identified the first C-9/C-10 link between fragments **A** and **C**, and an HMBC correlation observed between the fragment **A** methyl resonance at δ 0.80 (Me-23) and the fragment **C** methylene carbon resonance at δ 46.7 (C-22) identified a second C-11/C-22 connection between fragments **A** and **C**, which generated the final ring required by the molecular formula. Evidence for the C-6/C-7 linkage shown in Figure 1 (**A**–**D**) came from the observation of HMBC correlations between the H-5/H-5′ proton resonances at δ 2.02 and 2.40 and the C-7 olefinic carbon resonance at δ 138.5 and between the H-8 olefinic resonance at δ 5.03 and the C-6 methine resonance at δ 41.7. An HMBC correlation between the fragment **A** oxymethine proton resonance at δ 5.44 (H-13) and the acetyl carbonyl resonance at δ 169.5 (C-26) showed that the C-13 oxymethine oxygen atom was acetylated. A COSY correlation between the fragment **C** oxymethine proton resonance at δ 3.93 (H-9) and a proton resonance at δ 0.37 (OH-9), that was not correlated to a carbon resonance in the HSQC spectrum, revealed that the oxygen atom was part of an alcohol functionality, completing the constitution of **14**.

Coupling constant and ROESY data identified the relative configuration of anvilone A (**14**). The H-13 resonance was a dt with J = 3.8 and 11.2 Hz indicating that both H-13 and H-14 were axial, and the H-10 resonance was a doublet with J = 8.9 Hz consistent with a diaxial coupling with H-9. ROESY correlations observed between H-13 (δ 5.44) and both Me-23 (δ 0.80) and Me-24 (δ 0.96), between H-9 (δ 3.93) and both of Me-23 and Me-24, and between H-10 (δ 0.82) and H-14 (δ 1.21) confirmed that H-9, H-10, H-13, H-14, Me-23, and Me-24 were all axial, which established the relative configuration of the tricyclic fragment of **14** as shown in Figure 1 panel **e**. It was not possible to determine the relative configuration of fragments **A** and **B** in **14** from the NMR data.

Anvilone B (**15**) was isolated as a white powder that gave a $[M + Na]^+$ ion in the ESITOFHRMS spectrum at m/z 509.2885 appropriate for a molecular formula of $C_{29}H_{42}O_6$ (calcd for $C_{29}H_{42}O_6Na$ 509.2879) that required nine sites of unsaturation and differed from the molecular formula of anvilone A (**14**) by the addition of the elements $C_2H_2O_2$. The ^{13}C NMR spectrum of **15** contained four olefinic resonances (δ 128.3, C-8; 135.0, C-7; 138.5, C-3; 138.6, C-2) and three carbonyl resonances (δ 169.3, 1-OAc; 169.3, 13-OAC; 197.6, C-4) (Table 4 and Supporting Information) accounting for five sites of unsaturation, indicating that **15** had to be tetracyclic. Detailed analysis of the COSY and HMBC data recorded for anvilone B (**15**) revealed that it differed from anvilone A (**14**) simply by addition of a second acetoxy functionality in agreement with its molecular formula. COSY data showed that a deshielded methine at δ 5.26 (H-1) in the ^{1}H NMR spectrum of **15**, which was correlated to a carbon resonance at δ 66.7 (C-1) in the HSQC spectrum and to a carbon resonance at δ 169.3 (C-26) in the HMBC spectrum, replaced the H-1/H-1′ resonances at δ 1.67 and 1.80 in the ^{1}H NMR spectrum of **14**. Therefore, the new acetate functionality in **15** was located at C-1. A ROESY correlation observed between the methine proton resonances assigned to H-1 (δ 5.26) and H-6 (δ 2.18) in **15** demonstrated that the protons were *cis* as in all of the ansellones and alotaketals.

Anvilones A (**14**) and B (**15**) have the unprecedented tetracyclic "anvilane"" sesterterpenoid carbon skeleton named after Anvil Island, which is adjacent to the *Phorbas* sp. collecting sites in Howe Sound. Figure 2 shows a proposed biogenesis for the alotane (compounds **2**, **8**, and **9**), ansellane (compounds **3**–**6** and **10**–**13**), and anvilane sesterterpenoids (compounds **14** and **15**) that have been isolated from the British Columbia *Phorbas* sp. The proposal suggests that the biogenesis of the ansellane and anvilane skeletons proceeds through similar alotane intermediates (**I** or **II**) before diverging. Presumption of a common biogenesis for alotaketal C (**2**), ansellone A (**3**), ansellone C (**5**), and the anvilones A (**14**) and B (**15**) (see Figure 2) leads to the assignment of the absolute configurations 6*R*, 9*R*, 10*S*, 11*R*, 13*S*, 14*S*, 15*R* for **14** and

DOI: 10.1021/acs.joc.6b02312
J. Org. Chem. 2016, 81, 11324–11334

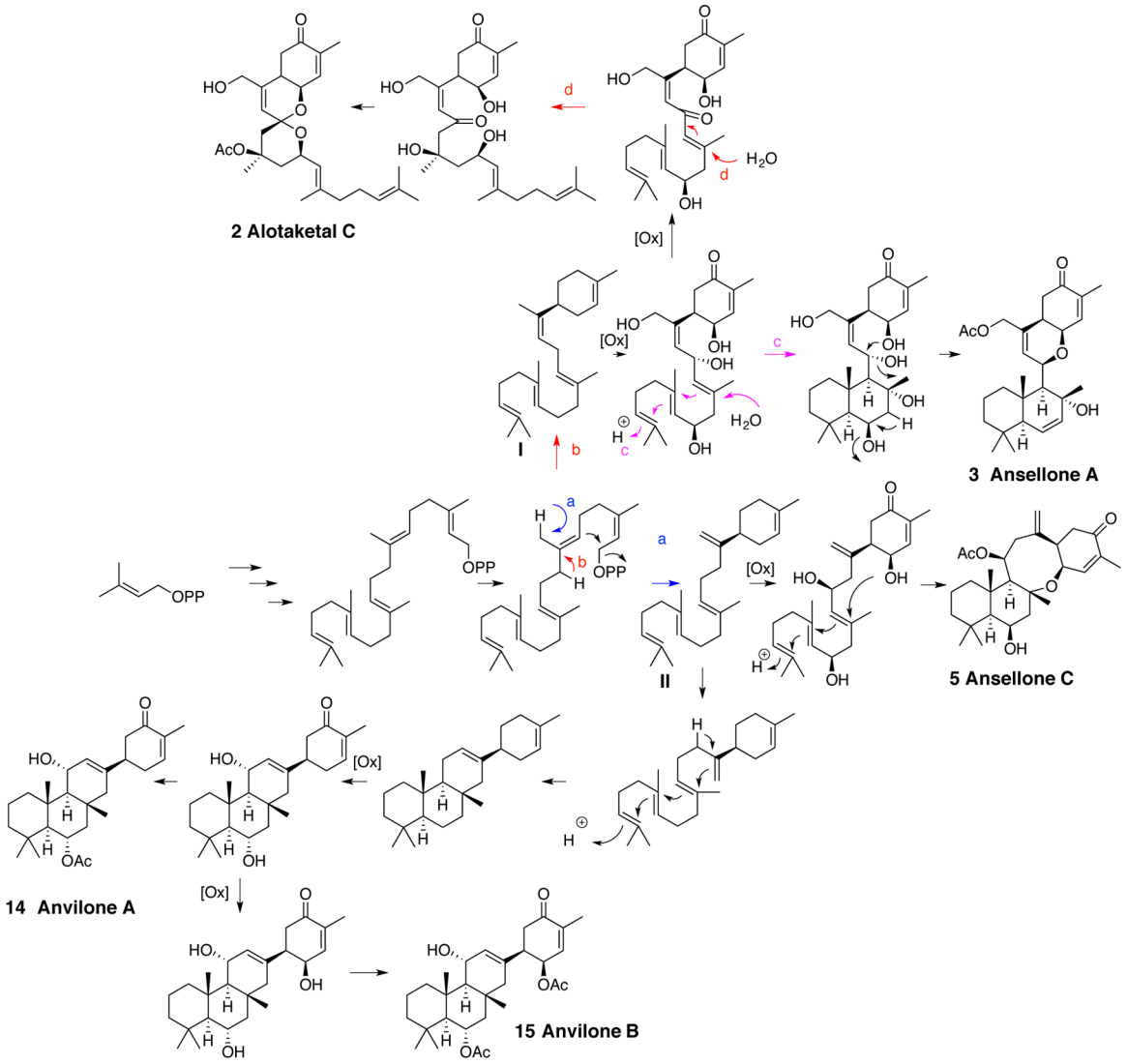

Figure 2. Proposed biogenesis of alotaketals, ansellones, and anvilones.

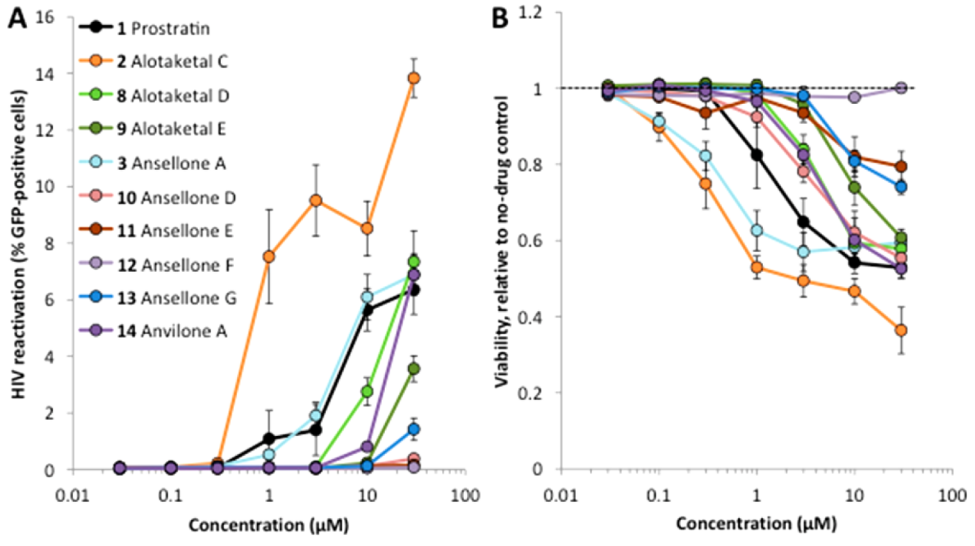

Figure 3. Effects of sesterterpenoids on HIV-1 provirus/GFP expression (A) and viability (B) of J-Lat 9.2 cells.

1*R*,6*R*,9*R*,10*S*,11*R*,13*S*,14*S*,15*R* for **15** that are shown in the drawings.

HIV-1 Latency Reversal by the *Phorbas* Sesterterpenoids. To investigate the potential effects of sesterterpenoids

DOI: 10.1021/acs.joc.6b02312
J. Org. Chem. 2016, 81, 11324−11334

on HIV-1 latency reversal, we used the established J-Lat 9.2 GFP-reporter CD4+ T cell line, which encodes a noninfectious (Δenv/Δnef) proviral genome.[7] Briefly, J-Lat cells were treated with sesterterpenoids and/or control LRAs for 24 h, and GFP protein, a marker of proviral gene expression, was measured by flow cytometry. In parallel, we also assessed cell viability by measuring the percentage of cells displaying normal forward- and side-scatter parameters in LRA-treated cells compared to cultures treated with 0.1% DMSO vehicle control.[12] Effects of sesterterpenoids on latent HIV-1 gene expression and J-Lat cell viability are summarized in Figure 3 and Table SI1 (Supporting Information). The most potent sesterterpenoid, **2** (alotaketal C), induced GFP expression in up to 13.8 ± 2.2% of J-Lat cells, or approximately 2.1-fold over the control LRA prostratin at the same concentration (30 μM; Figure 3A). Similar results were observed in cells treated with **1**−**3** and stained with a fluorescent antibody targeting the viral $p24^{Gag}$ protein (data not shown), confirming that these compounds induce viral protein production in addition to GFP. Furthermore, the toxicity of most sesterterpenoids that induced proviral gene expression was similar to that of prostratin (Figure 3B and Table SI1 Supporting Information), although **2** was more toxic to J-Lat cells (CC_{50} = 11.0 ± 7.8 μM). Taken together, multiple sesterterpenoids function as LRAs with activities comparable to that of control LRA prostratin in this cell culture model.

When added in combination, LRAs that act through different mechanisms are frequently observed to induce synergistic effects on proviral gene expression, while LRAs acting through similar pathways display only additive or weaker effects.[13−15] To investigate whether *Phorbas* sesterterpenoids may activate latent HIV-1 infection using similar mechanisms as established LRAs, we first treated J-Lat cells with selected sesterterpenoids at 1−30 μM for 24 h in the presence or absence of control LRAs with different known mechanisms of action including TNFα (pro-inflammatory cytokine), panobinostat (HDAC inhibitor), or prostratin (PKC activator) (Table SI2, Supporting Information).[5] In these studies, J-Lat cells treated with sesterterpenoids induced GFP expression in 3.0−9.2% of cells. Similarly, treatment of J-Lat cells with 10 ng/mL TNFα, 0.3 μM panobinostat, or 10 μM prostratin induced GFP expression in 13.2 ± 6.1, 15.2 ± 4.6, and 6.8 ± 2.9% of cells, respectively (Table SI2, Supporting Information). However, cells treated with sesterterpenoids plus TNFα or panobinostat induced GFP expression in 46.3−64.6% of cells, which is substantially more than expected for additive responses and demonstrates statistically significant levels of synergism using the previously described Bliss independence model.[13,14] In contrast, cells treated with sesterterpenoids plus prostratin induced GFP expression in only 9.2−13.8% of cells, which is more consistent with additive effects. These results suggest that sesterterpenoids induce HIV-1 proviral gene expression by mechanisms resembling those of prostratin.

To investigate further whether sesterterpenoids, like prostratin, may act as PKC agonists, we treated cells with sesterterpenoids or control LRAs for 24 h with or without the pan-PKC inhibitors GÖ-6983 and RO-31-8220 (Table SI3, Supporting Information).[16] While neither 1 μM of GÖ-6983 nor RO-31-8220 inhibited GFP expression in the presence of TNFα or panobinostat, both inhibited >85% of GFP expression induced by prostratin. As with prostratin, both PKC inhibitors also inhibited >85% of GFP expression induced by all tested sesterterpenoids, suggesting that sesterterpenoids, like prostratin, induce provirus expression through PKC activation pathways.

CONCLUSIONS

Compounds **2**−**15** isolated from the B.C. *Phorbas* sp. in this study are a family of highly functionalized sesterterpenoids that have the alotane (**2**, **8**, and **9**),[17] ansellane (**3**−**6** and **10**−**13**),[8,10] *seco*-ansellane (**7**),[8] and anvilane (**14** and **15**) carbon skeletons. The ansellane, *seco*-ansellane, and anvilane skeletons have so far only been found in metabolites isolated from this particular *Phorbas* sp. A biogenetic proposal for the formation of the alotane, ansellane, and anvilane skeletons is shown in Figure 2. It suggests that the new tetracyclic anvilane skeleton encountered in anvilones A (**14**) and B (**15**) is formed by two separate cyclization reactions on the linear precursor geranylfarnesyl pyrrophosphate. One of the cyclizations is initiated by the ionization of the C-1 allylic pyrrophosphate group leading to a cyclohexene ring, and the second cyclization is initiated by protonation of the $\Delta^{18,19}$ alkene to generate a 6,6,6 tricyclic fragment to form conjoint ring systems. Among this family of new sesterterpenoids, ansellone F (**12**) is of particular interest because it contains a rare 1,2−3,4-bis-epoxydecalin substructure that to the best of our knowledge has only been previously found in sesquiterpenoids isolated from leaves of the medicinal plant *Laurus nobilis*.[18]

Several of the *Phorbas* sp. sesterterpenoids were found to activate HIV-1 expression in a cell line model of latent HIV-1 reservoirs. Figure 3A shows that alotaketal C (**2**) gives ∼7% HIV-1 activation at a concentration of <1 μM, whereas the control LRA prostratin (**1**) gives ∼7% reactivation only at 30 μM, where alotaketal C (**2**) gives ∼14% HIV-1 activation, indicating that alotaketal C (**2**) is substantially more potent than prostratin (**1**). Figure 3B shows that alotaketal C (**2**) is also more toxic than prostratin (**1**), and the toxicity and efficacy profiles of the two compounds parallel each other. Ansellone A (**3**), alotaketal D (**8**), and anvilone A (**14**) were found to have LRA profiles that also resemble the control prostratin (**1**), while the other *Phorbas* sp. sesterterpenoids were only weakly active or inactive at a concentration of 30 μM (Figure 3 and Table SI1, Supporting Information). Combining alotaketal C (**2**) and other active *Phorbas* sesterterpenoids with known LRAs and inhibitors of PKC (Tables SI2 and SI3, Supporting Information) has shown that the *Phorbas* sesterterpenoids are most likely to be PKC activators. Similar to prostratin, they can synergize with other LRAs to activate latent HIV-1 gene expression, in some cases, in over 60% of cells (Table SI2, Supporting Information).

The alotaketals have been previously shown to potently activate the cAMP signaling pathway[18] and because they contain an enone substructure that is a potential Michael acceptor, they might be "pan assay interference compounds" (PAINS)[19] as a consequence of indiscriminate covalent binding to protein targets. However, alotaketal D (**8**) that has no enone is just as active as prostratin (**1**) at 30 μM, and conversely, several of the sesterterpenoids (**4**−**7** and **10**−**12**) that contain the enone functionality are inactive at 30 μM, demonstrating that simple covalent binding via the enone is not responsible for the LRA properties of these sesterterpenoids. In addition, a single change in the configuration at C-11 in ansellone E (**11**) renders it inactive at 30 μM, even though the epimer ansellone A (**3**) is as active as prostratin (**1**), and hydroxylation in the side chain of alotaketal E (**9**) dramatically reduces its activity

DOI: 10.1021/acs.joc.6b02312
J. Org. Chem. 2016, 81, 11324−11334

relative to alotaketal C (**2**). Therefore, the structural requirements for LRA in this family are quite subtle.

Several plant diterpenoids including prostratin, DPP (12-deoxyphorbol-13-phenylacetate), ingenol esters, gnidimacrin, and the stelleralides have been reported to activate latent HIV-1 reservoirs and have attracted attention as drug candidates for the "shock and kill" approach to a sterilizing treatment for infection.[5,6,20] Alotaketal C (**2**), alotaketal D (**8**), ansellone A (**3**), and anvilone A (**14**) are the first sesterterpenoids known to be agonists of PKC and able to activate latent HIV-1 reservoirs. Alotaketal C (**2**) is more potent than prostratin (**1**), but it is also more toxic. A recent study has shown that simple semisynthetic modification of natural ingenol esters enhanced their LRA potency and reduced their toxicity, demonstrating that SAR-driven improvement in therapeutic index is possible in these terpenoid families.[21] Two total syntheses of alotaketal A have been reported, which provide access to this scaffold and analogues for SAR.[22,23] Therefore, the *Phorbas* sesterterpenoids **2**, **3**, **8**, and **14** reported herein represent a new set of terpenoid scaffolds that are interesting lead structures for SAR-driven development of LRA cell biology tools and drug candidates.

EXPERIMENTAL SECTION

General Experimental Methods. The ^{1}H and ^{13}C NMR spectra were recorded on a 600 MHz spectrometer with a 5 mm cryoprobe. ^{1}H chemical shifts are referenced to residual C_6D_6 (δ 7.16), and ^{13}C chemical shifts are referenced to the C_6D_6 solvent peak (δ 128.4 ppm). Low- and high-resolution MS were recorded using ESI ionization and a TOF mass analyzer. Merck Type 5554 Si gl plates and Whatman MKC18F plates were used for analytical thin-layer chromatography. All solvents used for HPLC were HPLC grade.

Reagents. TNFα, prostratin, GÖ-6983, and RO-31-8220 were purchased from Sigma. Panobinostat was purchased from Selleck Chemicals (Houston, TX). p24^{Gag} antibody KC57-RD1 was purchased from Beckman Coulter. The following reagent was obtained from the NIH AIDS Reagent Program, Division of AIDS, NIAID, NIH: J-Lat Full Length Cells (9.2) (fom Dr. Eric Verdin).[7]

Animal Material. Specimens of the *Phorbas* sp. were collected on multiple occasions by hand using SCUBA on rocky shorelines near Ansell Point and Anvil Island in Howe Sound, British Columbia. The sponge was identified by Nicole J. de Voogd,[10] and a voucher specimen (code no.MNH POR. 5227) has been deposited at The Netherlands Centre for Biodiversity Naturalis, Leiden, The Netherlands. Freshly collected *Phorbas* sp. specimens were frozen for storage.

Extraction and Isolation. The frozen sponge (222 g) was extracted repeatedly with MeOH (3 × 150 mL) at room temperature. The combined methanolic extracts were concentrated in vacuo to afford 900 mg of brown solid. The extract was fractionated between H_2O (100 mL) and EtOAc (3 × 50 mL). The EtOAc partition was evaporated under reduced pressure and chromatographed on a Sephadex LH-20 column with 4:1 MeOH/CH_2Cl_2 as eluent to give six fractions A–F. Fraction B (200.1 mg) was chromatographed on a Si gel column using a gradient from 100% hexanes to 100% EtOAc to give 13 fractions BA-BM. Anvilone A (**14**) was obtained from fraction BG (10.7 mg) via C_{18} reversed-phase HPLC with 13:7 MeCN/H_2O as eluent. Ansellone D (**10**) was isolated from fraction BH (87.7 mg) by C_{18} reversed-phase HPLC using 1:1 MeCN/H_2O as eluent.

Another batch of fresh sponge (330 g) was collected and extracted repeatedly with MeOH (3 × 200 mL) at room temperature. The MeOH extracts were combined and concentrated in vacuo to afford 1.5 g of brown solid. After partition between H_2O (200 mL) and EtOAc (3 × 100 mL), the EtOAc fraction was subjected to Sephadex LH-20 column chromatography in 4:1 MeOH/CH_2Cl_2 to give fractions A–K. Fraction D (496 mg) was further fractionated by silica gel chromatography using a gradient from 100% hexanes to 100% EtOAc to give fractions DA-DR. Fractions DK, DL, DM, and DR were purified by C_{18} reversed-phase HPLC with 9:11 MeCN/H_2O as eluent to give the following compounds.

*Alotaketal D (**8**):* white powder (0.5 mg); $[\alpha]_D^{25}$ −5.4 (*c* 0.70 CD_2Cl_2); UV (MeOH) λ_{max} (log ε) 231.5 nm (5.09); ^{13}C NMR and ^{1}H NMR, see Table 1; positive-ion ESITOFHRMS [M + Na]$^+$ *m*/*z* 525.2827 (calcd for $C_{29}H_{42}O_7Na$, 525.2828).

*Alotaketal E (**9**):* white powder (0.5 mg); $[\alpha]_D^{25}$ +2.2 (*c* 0.005 CH_2Cl_2); UV (MeCN–H_2O 1:1) λ_{max} (log ε) 229 nm; ^{13}C NMR and ^{1}H NMR, see Table 1; positive-ion ESITOFHRMS [M + Na]$^+$ *m*/*z* 513.2452 (calcd for $C_{27}H_{38}O_8Na$, 513.2464).

*Ansellone D (**10**):* colorless powder (0.4 mg); $[\alpha]_D^{25}$ −8.8 (*c* 0.08 CD_2Cl_2); UV (MeOH) λ_{max} (log ε) 227.2 nm (4.08); ^{13}C NMR, see Table 2; ^{1}H NMR, see Table 3; positive-ion ESITOFHRMS [M + Na]$^+$ *m*/*z* 479.2778 (calcd for $C_{28}H_{40}O_5Na$, 479.2773).

*Ansellone E (**11**):* white powder (0.5 mg); $[\alpha]_D^{25}$ −5.4 (*c* 0.005 CH_2Cl_2); UV (MeCN–H_2O 4:1) λ_{max} (log ε) 228 nm (4.66); ^{13}C NMR, see Table 2; ^{1}H NMR, see Table 3; positive-ion ESITOFHRMS [M + Na]$^+$ *m*/*z* 465.2615 (calcd for $C_{27}H_{38}O_5Na$, 465.2617).

*Ansellone F (**12**):* white powder (1.0 mg); $[\alpha]_D^{25}$ −10.4 (*c* 0.005 CH_2Cl_2); UV (MeCN–H_2O 3:2) λ_{max} (log ε) 227 nm; ^{13}C NMR, see Table 2; ^{1}H NMR, see Table 3; positive-ion ESITOFHRMS [M + Na]$^+$ *m*/*z* 479.2403 (calcd for $C_{27}H_{36}O_6Na$, 479.2410).

*Ansellone G (**13**):* white powder (0.5 mg); $[\alpha]_D^{25}$ −30.5 (*c* 0.02 CD_2Cl_2); UV (MeOH) λ_{max} (log ε) 234.3 nm (4.89); ^{13}C NMR, see Table 2; ^{1}H NMR, see Table 3; positive-ion ESITOFHRMS [M + Na]$^+$ *m*/*z* 479.2409 (calcd for $C_{27}H_{36}O_6Na$, 479.2410).

*Anvilone A (**14**):* colorless powder (2.0 mg); $[\alpha]_D^{25}$ +3.2 (c 0.16 CD_2Cl_2); UV (MeOH) λ_{max} (log ε) 236.6 nm (4.66); ^{13}C NMR and ^{1}H NMR, see Table 4; positive-ion ESITOFHRMS [M + Na]$^+$ *m*/*z* 451.2823 (calcd for $C_{27}H_{40}O_4Na$, 451.2824).

*Anvilone B (**15**):* white powder (0.8 mg); $[\alpha]_D^{25}$ −7.6 (c 0.01 CH_2Cl_2); UV (MeCN–H_2O 1:1) λ_{max} (log ε) 232 nm; ^{13}C NMR and ^{1}H NMR, see Table 4; positive-ion ESITOFHRMS [M + Na]$^+$ *m*/*z* 509.2885 (calcd for $C_{29}H_{42}O_6Na$, 509.2879).

Cell Culture. J-Lat 9.2 cells were maintained in R10+ medium [RPMI-1640 with HEPES and L-Glutamine (Lonza), 10% fetal calf serum, 100 U/mL of penicillin, and 100 μg/mL of streptomycin (Sigma)] at 37 °C and 5% CO_2. Cells were resuspended in fresh R10+ to a concentration of 10^6 cells/mL, and 2 × 10^5 cells were seeded into 96-well plates with compounds (resuspended in DMSO) or 0.1 or 0.3% DMSO vehicle control in duplicate. Positive control substances used in the assay included 10 ng/mL TNF alpha (cytokine), 0.3 μM panobinostat (HDAC inhibitor), and 10–30 μM prostratin (PKC activator). In no case did the final concentration of DMSO in cell cultures exceed 0.3%, which in turn did not affect GFP expression or cellular toxicity compared to cells lacking DMSO treatment (data not shown). Cells were incubated at 37 °C and 5% CO_2 for an additional 24 h. Five thousand or 15000 cells from each culture were measured for cell toxicity and GFP expression by flow cytometry.

Data Analysis. Flow cytometry data were analyzed using FlowJo v. 8.8.7 software (FlowJo LLC, Ashland, OR). Cell toxicity was calculated as the relative percentage of cells displaying characteristic forward- and side-scatter parameters compared to control cultures incubated with 0.1% DMSO vehicle control. Background GFP expression in control cultures was set at 0.05% GFP-positive cells. Results are reported as the mean ± s.e.m. from at least three independent experiments. CC_{50} values for each compound were calculated from at least four concentrations.

Measures of synergy in LRA combinations were performed using the Bliss independence model as described previously.[13] Statistical analyses were performed using Student's unpaired *t* test, with a *p* value < 0.05 plus a Bonferroni correction to adjust for multiple comparisons considered significant.

ASSOCIATED CONTENT

Supporting Information

The Supporting Information is available free of charge on the ACS Publications website at DOI: 10.1021/acs.joc.6b02312.

DOI: 10.1021/acs.joc.6b02312
J. Org. Chem. 2016, 81, 11324–11334

1D and 2D NMR spectra for sesterterpenoids **8**−**15** and tables of biological activity data for compounds **1**−**15** (PDF)

AUTHOR INFORMATION

Corresponding Author

*E-mail: raymond.andersen@ubc.ca.

Notes

The authors declare no competing financial interest.

ACKNOWLEDGMENTS

Financial support was provided by grants from the Natural Sciences and Engineering Research Council of Canada (to RJA) and the Canadian Institutes for Health Research (HIG-133050, to MAB), and the International Development Research Centre (IDRC) Small Grants Program (to IT). Mike LeBlanc assisted the collection of the *Phorbas* sp. MAB holds a Canada Research Chair in Viral Pathogenesis and Immunity.

REFERENCES

(1) Chun, T. W.; Moir, S.; Fauci, A. S. *Nat. Immunol.* **2015**, *16*, 584−589.

(2) Archin, N. M.; Sung, J. M.; Garrido, C.; Soriano-Sarabia, N.; Margolis, D. M. *Nat. Rev. Microbiol.* **2014**, *12*, 750−764.

(3) Cary, D. C.; Fujinaga, K.; Peterlin, B. M. *J. Clin. Invest.* **2016**, *126*, 448−454.

(4) Archin, N. M.; Margolis, D. M. *Curr. Opin. Infect. Dis.* **2014**, *27*, 29−35.

(5) Xing, S.; Siliciano, R. F. *Drug Discovery Today* **2013**, *18*, 541−551.

(6) Rasmussen, T. A.; Lewin, S. R. *Curr. Opin. HIV AIDS* **2016**, *11*, 394−401.

(7) Jordan, A.; Bisgrove, D.; Verdin, E. *EMBO J.* **2003**, *22*, 1866−1877.

(8) Daoust, J.; Chen, M.; Wang, M.; Williams, D. E.; Chavez, M. A. G.; Wang, Y. A.; Merchant, C. E.; Fontana, A.; Kieffer, T. J.; Andersen, R. J. *J. Org. Chem.* **2013**, *78*, 8267−8273.

(9) Analysis of the NMR data obtained for the reisolated alotaketal C (**2**) (Table 1 and Supporting Information), which was identical to the originally reported data, confirmed that it has the $\Delta^{18,19}$ alkene correctly shown in **2** above and not the $\Delta^{19,20}$ alkene incorrectly drawn in ref 8.

(10) Daoust, J.; Fontana, A.; Merchant, C. E.; de Voogd, N. J.; Patrick, B. O.; Kieffer, T. J.; Andersen, R. J. *Org. Lett.* **2010**, *12*, 3208−3211.

(11) Rho, J.-R.; Hwang, B. S.; Sim, C. J.; Joung, S.; Lee, H.-Y.; Kim, H.-J. *Org. Lett.* **2009**, *11*, 5590−5593.

(12) Tietjen, I.; Ntie-Kang, F.; Mwimanzi, P.; Onguéné, P. A.; Scull, M. A.; Idowu, T. O.; Ogundaini, A. O.; Meva'a, L. M.; Abegaz, B. M.; Rice, C. M.; Andrae-Marobela, K.; Brockman, M. A.; Brumme, Z. L.; Fedida, D. *PLoS One* **2015**, *10*, e0121099.

(13) Laird, G. M.; Bullen, C. K.; Rosenbloom, D. I. S.; Martin, A. R.; Durand, C. M.; Siliciano, J. D.; Siliciano, R. F. *J. Clin. Invest.* **2015**, *125*, 1901−1912.

(14) Jiang, G.; Mendes, E. A.; Kaiser, P.; Wong, D. P.; Tang, Y.; Cai, I.; Fenton, A.; Melcher, G. P.; Hildreth, J. E. K.; Thompson, G. R.; Wong, J. K.; Dandekar, S. *PLoS Pathog.* **2015**, *11*, e1005066.

(15) Darcis, G.; Kula, A.; Bouchat, S.; Fujinaga, K.; Corazza, F.; Ait-Ammar, A.; Delacourt, N.; Melard, A.; Kabeya, K.; Vanhulle, C.; Van Driessche, B.; Gatot, J. S.; Cherrier, T.; Pianowski, L. F.; Gama, L.; Schwartz, C.; Vila, J.; Burny, A.; Clumeck, N.; Moutschen, M.; De Wit, S.; Peterlin, B. M.; Rouzioux, C.; Rohr, O.; Van Lint, C. *PLoS Pathog.* **2015**, *11*, e1005063.

(16) Abreu, C. M.; Price, S. L.; Shirk, E. N.; Cunha, R. D.; Pianowski, L. F.; Clements, J. E.; Tanuri, A.; Gama, L. *PLoS One* **2014**, *9*, No. e0097257.

(17) Forestieri, R.; Merchant, C. E.; de Voogd, N. J.; Matainaho, T.; Kieffer, T. J.; Andersen, R. J. *Org. Lett.* **2009**, *11*, 5166−5169.

(18) Julianti, E.; Jang, K. H.; Lee, S.; Lee, D.; Mar, W.; Oh, K.-B.; Shin, J. *Phytochemistry* **2012**, *80*, 70−76.

(19) Pouliot, M.; Jeanmart, S. *J. Med. Chem.* **2016**, *59*, 497−503.

(20) Asada, Y.; Sukemori, A.; Watanabe, T.; Malla, K. J.; Yoshikawa, T.; Li, W.; Koike, K.; Chen, C.-H.; Akiyama, T.; Qian, K.; Nakagawa-Goto, K.; Morris-Natschke, S. L.; Lee, K.-H. *Org. Lett.* **2011**, *13*, 2904−2907.

(21) Pandeló José, D. P.; Bartholomeeusen, K.; da Cunha, R. D.; Abreu, C. M.; Glinski, J.; da Costa, T. B. F.; Rabay, A. F. M. B.; Filho, L. F. P.; Lech W. Dudycz, L. W.; Ranga, U.; Peterlin, B. M.; Pianowski, L. F.; Tanuri, A.; Aguiar, R. S. *Virology* **2014**, *462-463*, 328−339.

(22) Xuan, M.; Paterson, I.; Dalby, S. M. *Org. Lett.* **2012**, *14*, 5492−5495.

(23) Huang, J.; Yang, J. R.; Zhang, J.; Yang, J. *J. Am. Chem. Soc.* **2012**, *134*, 8806−8809.

DOI: 10.1021/acs.joc.6b02312
J. Org. Chem. 2016, 81, 11324−11334